



LUND UNIVERSITY

Structure-Activity Studies and Therapeutic Potential of Host Defense Peptides of Human Thrombin

Kasetty, Gopinath; Papareddy, Praveen; Kalle, Martina; Rydengård, Victoria; Mörgelin, Matthias; Albiger, Barbara; Malmsten, Martin; Schmidtchen, Artur

Published in:
Antimicrobial Agents and Chemotherapy

DOI:
[10.1128/AAC.01515-10](https://doi.org/10.1128/AAC.01515-10)

2011

[Link to publication](#)

Citation for published version (APA):

Kasetty, G., Papareddy, P., Kalle, M., Rydengård, V., Mörgelin, M., Albiger, B., Malmsten, M., & Schmidtchen, A. (2011). Structure-Activity Studies and Therapeutic Potential of Host Defense Peptides of Human Thrombin. *Antimicrobial Agents and Chemotherapy*, 55(6), 2880-2890. <https://doi.org/10.1128/AAC.01515-10>

Total number of authors:
8

General rights

Unless other specific re-use rights are stated the following general rights apply:
Copyright and moral rights for the publications made accessible in the public portal are retained by the authors and/or other copyright owners and it is a condition of accessing publications that users recognise and abide by the legal requirements associated with these rights.

- Users may download and print one copy of any publication from the public portal for the purpose of private study or research.
- You may not further distribute the material or use it for any profit-making activity or commercial gain
- You may freely distribute the URL identifying the publication in the public portal

Read more about Creative commons licenses: <https://creativecommons.org/licenses/>

Take down policy

If you believe that this document breaches copyright please contact us providing details, and we will remove access to the work immediately and investigate your claim.

LUND UNIVERSITY

PO Box 117
221 00 Lund
+46 46-222 00 00

Structure-Activity Studies and Therapeutic Potential of Host Defense Peptides of Human Thrombin

Gopinath Kasetty,¹ Praveen Papareddy,¹ Martina Kalle,¹ Victoria Rydengård,¹ Matthias Mörgelin,² Barbara Albiger,¹ Martin Malmsten,³ and Artur Schmidtchen^{1*}

Division of Dermatology and Venereology¹, Division of Infection Medicine², Department of Clinical Sciences, Lund University, Biomedical Center, Tornavägen 10, SE-22184 Lund, Department of Pharmacy, Uppsala University³, SE-751 23, Uppsala, Sweden

Corresponding author. Mailing address: Division of Dermatology and Venereology, Department of Clinical Sciences, Lund University, Biomedical Center, Tornavägen 10, SE-22184 Lund, Sweden. Phone: +46 46 2224522. E-mail: artur.schmidtchen@med.lu.se.

Abstract

Peptides of the C-terminal region of human thrombin are released upon proteolysis, and identified in human wounds. In this study we wanted to investigate minimal determinants, as well as structural features, governing the antimicrobial and immunomodulating activity of this peptide region. Sequential amino acid deletions of the peptide GKYGFYTHVRLKKWIQKVIDQFGE (GKY25), as well as substitutions at strategic and structurally relevant positions were followed by analyses of antimicrobial activity against the Gram-negative *Escherichia coli* and *Pseudomonas aeruginosa*, the Gram-positive *Staphylococcus aureus* as well as the fungus *Candida albicans*. Furthermore, peptide effects on lipopolysaccharide (LPS)-, lipoteichoic acid-, or zymosan-induced macrophage activation were studied. The thrombin-derived peptides displayed length- and sequence-dependent antimicrobial as well as immunomodulating effects. A peptide length of at least 20 amino acids was required for effective anti-inflammatory effects in macrophage models, as well as optimal antimicrobial activity as judged by MIC assays. However, shorter (>12 amino acids) variants also displayed significant antimicrobial effects. A central K14 residue was important for optimal antimicrobial activity. Finally, one peptide variant, GKYGFYTHVRLKKWIQKVI (GKY20) exhibiting improved selectivity, i.e., low toxicity and a preserved antimicrobial as well as anti-inflammatory effect, showed efficiency in mouse models of LPS-shock and *P. aeruginosa* sepsis. The work defines structure-activity

relationships of C-terminal host defense peptides of thrombin, and delineates a strategy for selecting peptide epitopes of therapeutic interest.

Introduction

The extensive use of classical antibiotics has led to the emergence of increasing resistance among bacteria (10). In this perspective, cationic antimicrobial peptides (AMPs) are interesting since they provide a rapid and broad-spectrum response towards both Gram-negative and Gram-positive bacteria, as well as fungi. Although AMPs may influence bacteria in a multitude of ways (3), bacterial wall rupture seems to play a key role in the bactericidal action of most AMPs. During recent years it has become increasingly evident that many AMPs are multifunctional, also mediating various immunomodulatory roles and angiogenesis (7, 12, 14, 26, 45, 48), thus motivating the recent and broader definition host defense peptides (HDP) for these members of the innate immune system. The family of HDPs has recently been shown to encompass a diverse family of peptides, including proinflammatory and chemotactic chemokines (4), neuropeptides (3), peptide hormones (19, 27), growth factors (22), the anaphylatoxin peptide C3a (30, 34), and kininogen-derived peptides (11, 29, 39). We have previously shown that C-terminal peptides of thrombin constitute a novel class of HDPs, released upon proteolysis of thrombin *in vitro*, and detected in human wounds *in vivo*. These peptides exert antimicrobial effects against Gram-positive and Gram-negative bacteria, mediated by membrane lysis, as well as immunomodulatory functions, by inhibiting macrophage responses to bacterial lipopolysaccharide (31). In mice, they are protective against *P. aeruginosa* sepsis, as well as lipopolysaccharide-induced shock. Moreover, the thrombin-derived C-terminal peptides exhibit helical structures upon binding to lipopolysaccharide, and permeabilize liposomes, features typical of "classical" helical AMPs. These findings provide a novel link between the coagulation system and host-defense peptides, two fundamental biological systems activated in response to injury and microbial invasion. Although peptides were identified with these advantageous properties, however, the previous work provided no insight whether these peptides, or shorter sequences in these, are responsible for the effects observed. In the present study, we therefore set out to investigate minimal determinants, as well as structural features, governing the antimicrobial and immunomodulating activity of this peptide region.

MATERIALS AND METHODS

Peptides. Peptides were from Sigma-Genosys, generated by a peptide synthesis platform (PEPscreen®, Custom Peptide Libraries, Sigma Genosys). Prior to biological testing the PEPscreen peptides were diluted in dH₂O (5 mM stock), and stored at –20°C. This stock solution was used for the subsequent experiments. Selected peptides were synthesized by Biopeptide, San Diego, US. The purity (>95%) and molecular weight of these peptides was confirmed by both suppliers by mass spectral analysis (MALDI.TOF Voyager). LL-37 was from Innovagen AB, Lund, Sweden (purity >95%).

Microorganisms. *Escherichia coli* ATCC 25922, *Pseudomonas aeruginosa* ATCC 27853 *Staphylococcus aureus* ATCC 29213, and *Candida albicans* ATCC 90028 were obtained from the Department of Clinical Bacteriology at Lund University Hospital. Additional *S. aureus* clinical isolates were obtained from patients with skin infections.

Radial diffusion assay. Essentially as described earlier (20, 30) bacteria were grown to mid-logarithmic phase in 10 ml of full-strength (3% w/v) trypticase soy broth (TSB) (Becton-Dickinson, Cockeysville, MD). *Candida* was grown for 16 h at 28°C in 10 ml TSB medium to obtain yeast form organisms. The microorganisms were then washed once with 10 mM Tris, pH 7.4. Subsequently, 4 x 10⁶ bacterial colony forming units (cfu) or 3 x 10⁵ fungal cfu were added to 15 ml of the underlay agarose gel, consisting of 0.03% (w/v) TSB, 1% (w/v) low electroendosmosis type (EEO) agarose (Sigma, St Louis MO) and 0.02% (v/v) Tween 20 (Sigma) with or without 0.15M NaCl. The underlay was poured into a Ø 144 mm petri dish. After agarose solidification, 4 mm-diameter wells were punched and 6 µl of test sample was added to each well. Plates were incubated at 37°C for 3 hours to allow diffusion of the peptides. The underlay gel was then covered with 15 ml of molten overlay (6% TSB and 1% Low-EEO agarose in distilled H₂O). Antimicrobial activity of a peptide is visualized as a zone of clearing around each well after 18-24 hours of incubation at 37°C.

Viable-count analysis. *E. coli* ATCC 25922 bacteria were grown to mid-logarithmic phase in Todd-Hewitt (TH) medium (Becton and Dickinson, Maryland, USA). The microorganisms were then washed and diluted in 10 mM Tris, pH 7.4 containing 5 mM glucose. Following this, bacteria (50 µl; 2 x 10⁶ cfu/ml) were incubated, at 37°C for 2 hours, with the peptides

GKY25, GKY20, YTH20, or FYT20 (at 0.03, 0.06, 0.3, 0.6, 3, 6, 30, 60 μM) in 10 mM Tris, pH 7.4, 0.15 M NaCl, with or without 20% human citrate-plasma. In the experiments using 50% whole blood, *S. aureus* ATCC 29213 and *P. aeruginosa* ATCC 27853 bacteria (50 μl ; 2×10^8 cfu/ml) were incubated at 37°C for 1 hour in the presence of peptide at 60 (for *P. aeruginosa*) and 120 μM (*P. aeruginosa* and *S. aureus*). To quantify the bactericidal activity, serial dilutions of the incubation mixtures were plated on TH agar, followed by incubation at 37°C overnight and the number of cfu was determined. One hundred percent survival was defined as total survival of bacteria in the same buffer and under the same condition in the absence of peptide. Significance was determined using the statistical software SigmaStat (SPSS Inc., Chicago, IL, USA).

Hemolysis assay. For experiments in 50% blood, citrate-blood was diluted (1:1) with PBS. The cells were then incubated with end-over-end rotation for 1 h at 37°C in the presence of peptides (60 or 120 μM). Two per cent Triton X-100 (Sigma-Aldrich, St. Louis, USA) served as positive control. The samples were then centrifuged at 800 g for 10 min. The absorbance of hemoglobin release was measured at 540 nm and is expressed as % of TritonX-100 induced hemolysis. In the experiments with blood infected by bacteria, citrate-blood was diluted (1:1) with PBS. The cells were then incubated with end-over-end rotation for 1 h at 37°C in the presence of peptides (60 and 120 μM) and *S. aureus* (2×10^8 cfu/ml) or *P. aeruginosa* (2×10^8 cfu/ml) bacteria. For evaluation of hemolysis, samples were then processed as above.

Minimal inhibitory concentration assay (MIC). MIC analysis, defining the lowest concentration of the AMP that prevents microbial growth, was carried out by a microtiter broth dilution method (47). For determination of MIC, peptides were dissolved in 10 mM Tris, pH 7.4 at a concentration 5 times higher than the required range by serial dilutions from a stock solution. Twenty μl of each concentration was added to each corresponding well of a 96-well microtiter plate (polypropylene, Costar Corp., Cambridge, MA). Bacteria grown overnight in 3 % TSB was rinsed with Tris, pH 7.4, and diluted in refined LB medium to get a concentration of $\sim 1 \times 10^5$ cfu/ml. One hundred μl of bacterial solution in the refined LB medium was added to each well containing the test peptides. The plate was incubated at 37°C overnight. The MIC was taken as the concentration at which no visible bacterial growth was observed.

LPS effects on macrophages *in vitro*. RAW 264.7 macrophage cells (3.5×10^5) were seeded in 96-well tissue culture plates (Nunc, 167008) in phenol red-free DMEM (Gibco) supplemented with 10% FBS and antibiotics. Following 6 hours of incubation to permit adherence, cells were stimulated with 10 ng/ml *E. coli* LPS (0111:B4) or 10 μ g/ml *S. aureus* LTA (L2515) or 25 μ g/ml *Saccharomyces cerevisiae* Zymosan A (Z4250) (Sigma), with and without peptide of various doses. The levels of nitric oxide (NO) in culture supernatants were determined after 24 hours from stimulation using the Griess reaction (36). Briefly, nitrite, a stable product of NO degradation, was measured by mixing 50 μ l of culture supernatants with the same volume of Griess reagent (Sigma, G4410) and reading absorbance at 550 nm after 15 min. Phenol-red free DMEM with FBS and antibiotics were used as a blank. A standard curve was prepared using 0-80 μ M sodium nitrite solutions in ddH₂O.

Lactate dehydrogenase (LDH) assay. HaCaT keratinocytes were grown in 96-well plates (3000 cells/well) in serum free keratinocyte medium (SFM) supplemented with bovine pituitary extract and recombinant EGF (BPE-rEGF) (Invitrogen, USA) to confluency. The medium was then removed, and 100 μ l of the peptides investigated (at 60 μ M and 120 μ M, diluted in SFM/BPE-rEGF), was added in triplicates to different wells of the plate. The LDH based TOX-7 kit (Sigma-Aldrich, St Louis, USA) was used for quantification of LDH release from the cells. Results given represent mean values from triplicate measurements. Results are given as fractional LDH release compared to the positive control consisting of 1% Triton X-100 (yielding 100% LDH release).

MTT assay. Sterile filtered MTT (3-(4,5-dimethylthiazolyl)-2,5-diphenyl-tetrazolium bromide; Sigma-Aldrich) solution (5 mg/ml in PBS) was stored protected from light at -20°C until usage. HaCaT keratinocytes, 3000 cells/well, were seeded in 96-well plates and grown in serum free keratinocyte-SFM/BPE-rEGF medium to confluency. The peptides were then added at 60 μ M and 120 μ M. After incubation over night, 20 μ l of the MTT solution was added to each well and the plates incubated for 1 h in CO₂ at 37°C. The MTT containing medium was then removed by aspiration. The blue formazan product generated was dissolved by the addition of 100 μ l of 100% DMSO per well. The plates were then gently swirled for 10 min at room temperature to dissolve the precipitate. The absorbance was monitored at 550 nm, and results given represent mean values from triplicate measurements.

Fluorescence microscopy. For study of membrane permeabilization using the impermeant probe FITC, *E. coli* ATCC 25922 bacteria were grown to mid-logarithmic phase in TSB medium. The bacteria were washed and resuspended in either 10 mM Tris, pH 7.4, 10 mM glucose to yield a suspension of 1×10^7 cfu/ml. Hundred microliters of the bacterial suspension was incubated with 30 μ M of the respective peptides at 30°C for 30 min. Microorganisms were then immobilized on poly (L-lysine)-coated glass slides by incubation for 45 min at 30°C, followed by addition onto the slides of 200 μ l of FITC (6 μ g/ml) in the appropriate buffers and incubated for 30 min at 30°C. The slides were washed and bacteria were fixed by incubation, first on ice for 15 min, then in room temperature for 45 min in 4% paraformaldehyde. The glass slides were subsequently mounted on slides using Prolong Gold antifade reagent mounting medium (Invitrogen). For fluorescence analysis, bacteria were visualized using a Nikon Eclipse TE300 (Nikon, Melville, NY) inverted fluorescence microscope equipped with a Hamamatsu C4742-95 cooled CCD camera (Hamamatsu, Bridgewater, NJ) and a Plan Apochromat \times 100 objective (Olympus, Orangeburg, NY). Differential interference contrast (Nomarski) imaging was used for visualization of the microbes themselves.

Liposome preparation and leakage assay. Anionic DOPE/DOPG (75/25 mol/mol) liposomes were investigated regarding peptide-induced membrane disruption. DOPG (1,2-dioleoyl-*sn*-Glycero-3-phosphoglycerol, monosodium salt), and DOPE (1,2-dioleoyl-*sn*-Glycero-3-phosphoethanolamine) were from Avanti Polar Lipids (Alabaster, USA) and of >99% purity. The lipid mixture was dissolved in chloroform, after which solvent was removed by evaporation under vacuum overnight. Subsequently, 10 mM Tris buffer, pH 7.4, was added together with 0.1 M carboxyfluorescein (CF) (Sigma, St. Louis, USA). After hydration, the lipid mixture was subjected to eight freeze-thaw cycles, consisting of freezing in liquid nitrogen and heating to 60°C. Unilamellar liposomes of about $\text{\O}140$ nm were generated by multiple extrusions through polycarbonate filters (pore size 100 nm) mounted in a LipoFast miniextruder (Avestin, Ottawa, Canada) at 22°C. Untrapped CF was removed by two subsequent gel filtrations (Sephadex G-50, GE Healthcare, Uppsala, Sweden) at 22°C, with Tris buffer as eluent. CF release from the liposomes was determined by monitoring the emitted fluorescence at 520 nm from a liposome dispersion (10 mM lipid in 10 mM Tris, pH 7.4). An absolute leakage scale was obtained by disrupting the liposomes at the end of each

experiment through addition of 0.8 mM Triton X-100 (Sigma-Aldrich, St. Louis, USA). A SPEX-fluorolog 1650 0.22-m double spectrometer (SPEX Industries, Edison, USA) was used for the liposome leakage assay. Measurements were performed in triplicate at 37 °C.

CD-spectroscopy. The CD spectra of the peptides in solution were measured on a Jasco J-810 Spectropolarimeter (Jasco, U.K.). The measurements were performed at 37°C in a 10 mm quartz cuvet under stirring and the peptide concentration was 10 µM. The effect on peptide secondary structure of liposomes at a lipid concentration of 100 µM was monitored in the range 200-250 nm. The fraction of the peptide in α -helical conformation was calculated from the CD signal at 225 nm. 100% α -helix and 100% random coil references were obtained from 0.133 mM (monomer concentration) poly-L-lysine in 0.1 M NaOH and 0.1 M HCl, respectively (13, 42) For determination of effects of lipopolysaccharide on peptide structure, the peptide secondary structure was monitored at a peptide concentration of 10 µM, both in Tris buffer and in the presence of *E. coli* lipopolysaccharide (0.02 wt%) (*Escherichia coli* 0111:B4, highly purified, less than 1% protein/RNA, Sigma, UK). To account for instrumental differences between measurements the background value (detected at 250 nm, where no peptide signal is present) was subtracted. Signals from the bulk solution were also corrected for. Measurements were performed in triplicate at 37 °C.

LPS model *in vivo*. Male C57BL/6 mice (8-10 weeks, 22 +/- 5g),) were housed under standard conditions of light and temperature and had free access to standard laboratory chow and water. All experiments were approved by the Laboratory Animal Ethics Committee of Malmö/Lund. Mice were injected intraperitoneally (i.p.) with 18 mg *E. coli* 0111:B4 LPS (Sigma) per kg of body weight. Thirty minutes after LPS injection, 0.5 mg GKY20 or buffer alone was injected intraperitoneally into the mice. Survival and status was followed during seven days. For blood collection and histochemistry, mice were sacrificed 20 h after LPS challenge, and lungs were removed and fixed.

Cytokine assay. The cytokines IL-6, IL-10, MCP-1, INF- γ , and TNF- α were measured in plasma from mice subjected to LPS (with or without peptide treatment) using the Cytometric bead array; mouse inflammation kit (Becton Dickinson AB) according to the manufacturer's instructions.

Animal infection model. *P. aeruginosa* 15159 bacteria were grown to logarithmic phase (OD₆₂₀~0.5), harvested, washed in PBS, diluted in the same buffer to 2×10^8 cfu/ml, and kept on ice until injection. One hundred microliter of the bacterial suspension was injected i.p. into female C57/BL6 mice. Thirty minutes after the bacterial injection, 0.5 mg GKY20 or buffer alone was injected i.p. into the mice. In order to study bacterial dissemination to target organs spleen, liver and kidney were harvested, placed on ice, homogenized, and cfu determined. The P-value was determined using the Mann-Whitney U-test. Data from three independent experiments were pooled.

Tissue analyses. For scanning electron microscopy (SEM), specimens were washed with cacodylate buffer, and dehydrated with an ascending ethanol series from 50% (v/v) to absolute ethanol (10 min per step). The specimens were then subjected to critical-point drying in carbon dioxide, with absolute ethanol as intermediate solvent, mounted on aluminium holders, sputtered with 30 nm palladium/gold, and examined in a JEOL JSM-350 scanning electron microscope. For histological evaluation of lungs derived from the *in vivo* LPS-models in mice, tissues were embedded as above, sectioned and stained with hematoxylin and eosin by routine procedures (Histocenter, Gothenburg, Sweden).

Calculations. Relative hydrophobic moment (μ_{Hrel}) was calculated using the web-based algorithm found at <http://www.bbcm.univ.trieste.it/~tossi/HydroCalc/HydroMCalc.html>.

RESULTS

Previous x-ray crystallographic studies of intact thrombin have shown that the C-terminal region (HVFRLKKWIKVIDQFGE) adopts an α -helical conformation in the thrombin molecule (2). As an isolated peptide, on the other hand, this region adopts a dynamic random coil conformation in aqueous solution (31). Nevertheless, the peptide GKY25 (GKYGFYTHVFRLKKWIKVIDQFGE) has the ability to adopt a helical conformation in specific solvent environments, such as the presence of LPS (31). It is notable that the peptide contains a helix stabilizing N-cap motif of the C-terminal helix. Furthermore, the side chain of H8 (in GKY25) makes a hydrogen bond to the backbone amide three residues downstream

(R11). Of relevance for this peptide region is also the observation that a spacing of $i, i + 3$ or $i, i + 4$ between hydrophobic residues such as L, I, and W is known to stabilize helices with the latter spacing giving the strongest interaction (21). In order to evaluate minimal antimicrobial epitopes of GKY25, as well as determine the potential hemolytic effects of these shorter fragments, peptides sequentially truncated from either the C- or N-terminus were analyzed in RDA against *E. coli* as well as tested for hemolysis using human erythrocytes. As shown in Figure 1, bactericidal activities were retained for shorter fragments, as particularly noted for the C- and the simultaneously N- and C-terminally truncated peptides. In general, the presence of 0,15 M NaCl was slightly inhibitory on peptide antimicrobial activity. It is notable that the short N and C-terminally truncated 12-mer peptide, VFRLKKWIQKVI, containing the central "core", retained good bactericidal potency at high salt conditions (Fig. 1A). In general, peptides having lengths of above 18-20 amino acids displayed hemolytic effects at the concentration tested (60 μ M) (Fig. 1 A). The antimicrobial analyses were extended to the Gram-negative *P. aeruginosa*, the Gram-positive *S. aureus*, and the fungus *C. albicans* (Fig. 1 B). Apart from showing the broad spectrum activity of GKY25, the results illustrate that GKY-derived peptides of shorter length (down to 8-10 amino acid residues) retain most of their activity at the low salt conditions used. Hence, taken together, the results illustrate that hemolytic and antibacterial effects partly overlap, although there is a tendency that shorter peptide fragments of 15-20 amino acids retain good antimicrobial activity, yet relatively limited hemolysis. In order to further delineate some structural prerequisites determining activity, we synthesized 16-mer peptides based on the internal sequence THVFRLKKWIQKVIDQ ($z_{\text{net}} = +4$), encompassing the critical N- and C-cap motifs, but having the cationic R and K-residues sequentially replaced by S. It is notable that among the peptides having one K replaced ($z_{\text{net}} = 3$), the central K residue N-terminal of W appeared to be the most critical for antimicrobial activity, particularly against *S. aureus*. Introducing one more change in this peptide, again in the central part, and C-terminal of Q, almost completely abrogated the activity of the peptide (Fig. 2). Thus, the results indicate that the two central K residues adjacent to the evolutionary conserved WI sequence are particularly important for determining the antimicrobial activity of this region of the peptide.

Given the potent anti-endotoxic effects of GKY25, we next studied the length dependence of the anti-inflammatory effect in a macrophage model. As seen in Figure 3, the results showed that a peptide length of minimum 19-20 amino acids is required for complete

inhibition of LPS-mediated signalling. A similar dependence was observed for LTA- as well as zymosan-mediated NO-induction. Taken together, the results demonstrate a partial overlap between antimicrobial and anti-endotoxic activity, and indicate that successive truncations of GK Y25 may yield shorter peptides of a minimum size of 19-20 amino acids having preserved antimicrobial and immunomodulatory properties.

Next, we analyzed selected peptides corresponding to three major groups, i) peptides of 20 amino acids showing "dual" effects (exerting both antimicrobial activity in high salt and anti-inflammatory activity), ii) those only yielding antimicrobial effects in high salt (of 16 amino acids), and iii) those only showing activity in low salt buffers. MIC assays using various *E. coli* and *S. aureus* strains showed that only the 20-mer peptides, and particularly the C-terminally truncated GKYGFYTHVFRLKKWI (GKY20), and the N- and C-terminally truncated FYTHVFRLKKWIQKVIDQFG (FYT20) presented low MICs comparable to that of the parent GK Y25, as well as the benchmark peptide LL-37 (Fig. 4A). It was also noted that the pure FYT20 peptide displayed some turbidity when dissolved at 5 mM, likely illustrating the high hydrophobicity and amphipathicity of this particular peptide region. In order to further explore the effects of these peptides in relevant physiological environments, viable count assays in 0.15 M NaCl and in presence of 20% human plasma were performed (Fig. 4B). Whereas GKY20 showed similar antimicrobial activities in both environments, the N- and C-terminally truncated FYT20, as well as N-terminally truncated YTH20, were significantly inhibited, particularly in human plasma (Fig. 4B). Anti-endotoxin activity was probed for the truncated variants and compared with activity of the full-length GK Y25. In correspondence with the initial screening results, the 20-mer peptides showed anti-inflammatory activities at or below 10 μ M, in contrast to the shorter 16- and 12-mer variants. Interestingly, GKY16 still retained some activity at 50 μ M (Fig. 5A). At 10 μ M, the 20-mer peptide variants also inhibited LTA- and zymosan-induced NO-release from macrophages (Fig. 5B).

The 20-mer peptides all showed less hemolysis than the original GK Y25 peptide, as well as LL-37 (Fig. 6A), however, it was noted that the dose of GK Y25 required for permeabilization of erythrocytes significantly exceeded the MIC values (Fig. 4A), as well as the concentration required for efficient bacterial killing in the viable count assays (Fig. 4B). Likewise, the 20-mer variants affected viability to a lesser extent than GK Y25 as well as LL-37, although the LDH-release was similar. In the presence of serum, on the other hand, the 20-mers displayed no detectable permeabilization with either LDH release or MTT assay

(Fig. 6B). It was noted that both GKY25 and LL-37 showed some permeabilizing activity also in serum at 60 μ M (Fig. 6B). Analogously, permeabilization of human skin fibroblasts by the 20-mer peptides was largely absent at 60 μ M, in contrast to the findings obtained with GKY25 as well as LL-37 (Fig. 6C). In order to simultaneously explore hemolytic (Fig. 7A) as well as antimicrobial effects (Fig. 7B), of importance for subsequent *in vivo* studies, the two peptides GKY25 and GKY20 were added to human blood infected by *S. aureus* or *P. aeruginosa*. It was observed that the peptides, and particularly GKY20, displayed a significant selectivity, demonstrating almost complete eradication of *P. aeruginosa* and *S. aureus*, with little (\sim 5% or less) accompanying hemolysis, at a peptide dose of 120 μ M. Taken together, the combination of hemolysis results and permeabilization studies on HaCat keratinocytes as well as human fibroblasts indicate that the truncated peptides, and particularly GKY20, show reduced toxicity at doses above those needed for antimicrobial as well as anti-inflammatory effects.

Figure 8A shows that like GKY25, the 20-mer variants permeabilized *E. coli* cells, as visualized with the impermeant probe FITC. To further examine peptide-induced permeabilization of bacterial plasma membranes, *P. aeruginosa* and *S. aureus* was incubated with GKY20 at concentrations yielding complete bacterial killing (30 μ M), and analyzed by electron microscopy (Fig. 9B). Clear differences in morphology between peptide-treated bacteria and the control were demonstrated. The peptide caused local perturbations and breaks along *P. aeruginosa* and *S. aureus* plasma membranes, and intracellular material was found extracellularly. In order to obtain further structural and mechanistic information, we studied GKY25 (**GKYGFYTHVFR**LKKW**IQKVIDQFGE**), GKY20 (bold in previous sequence), as well as the epitope VFRLKKW**IQKVI** (VFR12, in italics), the latter retaining significant antimicrobial effects when compared with GKY20. As demonstrated in Figure 8C, the peptides showed mostly a random coil conformation in buffer. However, LPS induced a conformational change in all the three peptide variants. In contrast, as seen in the CD-spectrum (Fig. 8C), and depicted in Figure 8D, anionic liposomes significantly affected helix content only for GKY25. Despite this, GKY25 and GKY20 showed similar membrane disruptive effects on liposomes, and their activity in this context was significantly higher when compared with VFR12 (Fig. 8E), likely reflecting a lower entropy penalty for membrane insertion for these longer peptides compared to the shorter VFR12, in analogy to effects found previously, e.g., for cardin consensus peptides (37).

Taken together, the above studies demonstrated the possibility of maintaining desired antimicrobial and anti-inflammatory effects, while reducing peptide length and attenuating peptide toxicity. The peptide GK Y20, meeting prerequisites of little inhibition in plasma, reduced toxicity, as well as maintained MIC values and antiinflammatory effects, was selected in order to further investigate the potential therapeutic effectiveness *in vivo*. We therefore injected this peptide into mice infected intraperitoneally with *P. aeruginosa*. Compared to the controls, treatment with GK Y20 reduced bacterial numbers in the spleen, liver, and kidney of the animals (Fig. 9A). In a mouse model of LPS-induced shock, GK Y20 displayed a dramatic improvement on survival (Fig. 9B, left panel). The treated animals also showed recovery of weight (Fig. 9B, right panel). Analyses of platelet counts after 12 h showed that GK Y20 significantly increased platelets, indicative of reduced consumption in this particular LPS-model (Fig. 9C). Analyses of cytokines 20 hours after LPS injection showed significant reductions of proinflammatory IL-6, IFN- γ , TNF- α , and MCP-1, whereas an increase in anti-inflammatory IL-10 was observed (Fig. 9D). Furthermore, a marked reduction of inflammation and vascular leakage in the lungs of the GK Y20-treated animals was observed after histochemical evaluation of the lungs (Fig. 9E). Correspondingly, while SEM analyses of the lungs from LPS-treated animals demonstrated pulmonary leakage of protein and red blood cells (Fig. 10F), lungs of GK Y20-treated animals showed marked reductions of these LPS-induced effects. The results thus demonstrate the therapeutic potential of GK Y20 in these animal models of *P. aeruginosa* sepsis and LPS-induced shock.

DISCUSSION

Considering the increasing resistance problems against conventional antibiotics, a number of HDPs and peptidomimetics are currently undergoing clinical trials (6, 14, 16, 24). In most cases, trials are aimed at topical indications where direct microbicidal effects are utilized. Considering this property of AMPs, various strategies have been employed in order to optimize the therapeutic index including use of combinational library approaches (1), stereoisomers composed of D-amino acids (40) or cyclic D,L- α -peptides (8), QSAR and high-throughput based screening assays (9, 15, 18, 35, 44). Furthermore, a novel approach for boosting AMPs through end-tagging with hydrophobic oligopeptide stretches have recently been demonstrated (23, 32, 33, 41). The peptides were active *ex vivo* and *in vivo* in porcine *S. aureus* skin infection models, and in *P. aeruginosa* infected wound models (23,

32, 33, 41). Immunomodulatory peptides have recently gained much interest due to their capacity to selectively boost or down-regulate immune effectors during infection (17, 25, 26, 28, 43, 45). Naturally occurring peptide epitopes may show promise in a therapeutic setting considering low immunogenicity paired with the endogenous immunomodulatory activities described here. However, as shown in the present study on the thrombin-derived GKY25, a systematic analysis of epitopes with respect to size as well as sequence is required in order to define and select peptide regions with preferred activities with respect to efficiency and therapeutic index. The necessity of this approach is exemplified by the observation that even minor differences in selection of the active 20-mer region, yielded different activities with respect to inactivation by plasma, observed MIC values, as well as anti-inflammatory effects. It is also possible, that the GKY20 sequence could be used as a template in order to further define and possibly enhance the immunomodulatory activities of the peptide, a strategy successfully used for other peptides (6, 28). Finally, the results demonstrate that a concerted approach, utilizing not only experiments with erythrocytes in PBS, but also including results obtained in plasma and blood are required in order to better assess potential toxic effects of a given peptide.

Considering the endotoxin neutralizing activities, the mode of action GKY20 may involve binding to and neutralization of LPS, yielding inhibition of subsequent TLR-signaling, as described for other helical peptides (38). However, it is also possible that the peptide acts by additional mechanisms, which involve direct effects on host cells such as macrophages. In relation to this, it is notable that the 12-mer peptide VFR12, while showing binding and induction of a helical conformation in presence of LPS, was not able to block LPS effects in the macrophage model. As the latter requires a size of at least 19-20 amino acids, the results suggest that additional mechanisms, apart from direct LPS-binding, may contribute to the observed anti-endotoxin effects. Indeed, and in line with this reasoning, hydrophobically tagged peptides with high affinity for LPS (32, 33, 41) showed little anti-inflammatory effects in the macrophage models used here (data not shown). The possible mechanisms underlying the function of GKY20/GKY25 remain to be investigated but may include interactions with CD14, TLRs, or intracellular receptors.

As demonstrated here, peptides derived from natural HDPs, such as exemplified by GKY20, can be interesting since they retain the main properties of the parent molecule. Considering the significant anti-inflammatory effects, but modest direct antimicrobial activity of GKY20 *in vivo*, the potential use of this HDP may be in situations

characterized by excessive endotoxin loads and overactivation of various inflammatory pathways. For example, it is possible that peptide-mediated attenuation of excessive TLR-stimulation could be employed in targeting the hyperinflammatory stage during sepsis development (5, 46). Clearly, further investigations involving additional *in vivo* animal models of infection and septic shock, as well as toxicological analyses are mandated in order to further explore the potential of these HDPs as novel therapeutic candidates for clinical developments.

ACKNOWLEDGMENT

This work was supported by grants from the Swedish Research Council (projects 521-2009-3378, 7480, and 621-2003-4022), the Royal Physiographic Society in Lund, the Welanders-Finsen, Crafoord, Österlund, and Kock Foundations, Marianne and Marcus Wallenberg Foundation, XImmune AB, and The Swedish Government Funds for Clinical Research (ALF). Ms. Maria Baumgarten, Ms. Mina Davoudi and Ms. Lise-Britt Wahlberg are gratefully acknowledged for technical support.

REFERENCES

1. **Blondelle, S. E., and K. Lohner.** 2000. Combinatorial libraries: a tool to design antimicrobial and antifungal peptide analogues having lytic specificities for structure-activity relationship studies. *Biopolymers* **55**:74-87.
2. **Bode, W.** 2006. The structure of thrombin: a janus-headed proteinase. *Semin Thromb Hemost* **32 Suppl 1**:16-31.
3. **Brogden, K. A.** 2005. Antimicrobial peptides: pore formers or metabolic inhibitors in bacteria? *Nat Rev Microbiol* **3**:238-250.
4. **Cole, A. M., T. Ganz, A. M. Liese, M. D. Burdick, L. Liu, and R. M. Strieter.** 2001. Cutting edge: IFN-inducible ELR- CXC chemokines display defensin-like antimicrobial activity. *J Immunol* **167**:623-627.
5. **de Jong, H. K., T. van der Poll, and W. J. Wiersinga.** 2010. The systemic pro-inflammatory response in sepsis. *J Innate Immun* **2**:422-430.

6. **Easton, D. M., A. Nijnik, M. L. Mayer, and R. E. Hancock.** 2009. Potential of immunomodulatory host defense peptides as novel anti-infectives. *Trends Biotechnol* **27**:582-590.
7. **Elsbach, P.** 2003. What is the real role of antimicrobial polypeptides that can mediate several other inflammatory responses? *J Clin Invest* **111**:1643-1645.
8. **Fernandez-Lopez, S., H. S. Kim, E. C. Choi, M. Delgado, J. R. Granja, A. Khasanov, K. Kraehenbuehl, G. Long, D. A. Weinberger, K. M. Wilcoxon, and M. R. Ghadiri.** 2001. Antibacterial agents based on the cyclic D,L-alpha-peptide architecture. *Nature* **412**:452-455.
9. **Fjell, C. D., H. Jenssen, W. A. Cheung, R. E. Hancock, and A. Cherkasov.** 2011. Optimization of antibacterial peptides by genetic algorithms and cheminformatics. *Chem Biol Drug Des* **77**:48-56.
10. **French, G. L.** 2005. Clinical impact and relevance of antibiotic resistance. *Adv Drug Deliv Rev* **57**:1514-1527.
11. **Frick, I. M., P. Akesson, H. Herwald, M. Morgelin, M. Malmsten, D. K. Nagler, and L. Bjorck.** 2006. The contact system--a novel branch of innate immunity generating antibacterial peptides. *Embo J* **25**:5569-5578.
12. **Ganz, T.** 2003. Defensins: antimicrobial peptides of innate immunity. *Nat Rev Immunol* **3**:710-720.
13. **Greenfield, N., and G. D. Fasman.** 1969. Computed circular dichroism spectra for the evaluation of protein conformation. *Biochemistry* **8**:4108-4116.
14. **Hancock, R. E., and H. G. Sahl.** 2006. Antimicrobial and host-defense peptides as new anti-infective therapeutic strategies. *Nat Biotechnol* **24**:1551-1557.
15. **Hilpert, K., R. Volkmer-Engert, T. Walter, and R. E. Hancock.** 2005. High-throughput generation of small antibacterial peptides with improved activity. *Nat Biotechnol* **23**:1008-1012.
16. **Hirsch, T., F. Jacobsen, H. U. Steinau, and L. Steinstraesser.** 2008. Host defense peptides and the new line of defence against multiresistant infections. *Protein Pept Lett* **15**:238-243.
17. **Jenssen, H., and R. E. Hancock.** 2010. Therapeutic potential of HDPs as immunomodulatory agents. *Methods Mol Biol* **618**:329-347.
18. **Jenssen, H., T. Lejon, K. Hilpert, C. D. Fjell, A. Cherkasov, and R. E. Hancock.** 2007. Evaluating different descriptors for model design of antimicrobial peptides with enhanced activity toward *P. aeruginosa*. *Chem Biol Drug Des* **70**:134-142.

19. **Kowalska, K., D. B. Carr, and A. W. Lipkowski.** 2002. Direct antimicrobial properties of substance P. *Life Sci* **71**:747-750.
20. **Lehrer, R. I., M. Rosenman, S. S. Harwig, R. Jackson, and P. Eisenhauer.** 1991. Ultrasensitive assays for endogenous antimicrobial polypeptides. *J Immunol Methods* **137**:167-173.
21. **Luo, P., and R. L. Baldwin.** 2002. Origin of the different strengths of the (i,i+4) and (i,i+3) leucine pair interactions in helices. *Biophys Chem* **96**:103-108.
22. **Malmsten, M., M. Davoudi, B. Walse, V. Rydengard, M. Pasupuleti, M. Mörgelin, and A. Schmidtchen.** 2007. Antimicrobial peptides derived from growth factors. *Growth Factors* **25**:60-70.
23. **Malmsten, M., G. Kasetty, M. Pasupuleti, J. Alenfall, and A. Schmidtchen.** 2011. Highly Selective End-Tagged Antimicrobial Peptides Derived from PRELP. *PLoS One* **6**:e16400.
24. **Marr, A. K., W. J. Gooderham, and R. E. Hancock.** 2006. Antibacterial peptides for therapeutic use: obstacles and realistic outlook. *Curr Opin Pharmacol.* **6**:468-472
25. **Mookherjee, N., K. L. Brown, D. M. Bowdish, S. Doria, R. Falsafi, K. Hokamp, F. M. Roche, R. Mu, G. H. Doho, J. Pistolic, J. P. Powers, J. Bryan, F. S. Brinkman, and R. E. Hancock.** 2006. Modulation of the TLR-mediated inflammatory response by the endogenous human host defense peptide LL-37. *J Immunol* **176**:2455-2464.
26. **Mookherjee, N., D. N. Lippert, P. Hamill, R. Falsafi, A. Nijnik, J. Kindrachuk, J. Pistolic, J. Gardy, P. Miri, M. Naseer, L. J. Foster, and R. E. Hancock.** 2009. Intracellular receptor for human host defense peptide LL-37 in monocytes. *J Immunol* **183**:2688-2696.
27. **Mor, A., M. Amiche, and P. Nicolas.** 1994. Structure, synthesis, and activity of dermaseptin b, a novel vertebrate defensive peptide from frog skin: relationship with adenoregulin. *Biochemistry* **33**:6642-6650.
28. **Nijnik, A., L. Madera, S. Ma, M. Waldbrook, M. R. Elliott, D. M. Easton, M. L. Mayer, S. C. Mullaly, J. Kindrachuk, H. Jensen, and R. E. Hancock.** 2010. Synthetic cationic peptide IDR-1002 provides protection against bacterial infections through chemokine induction and enhanced leukocyte recruitment. *J Immunol* **184**:2539-2550.
29. **Nordahl, E. A., V. Rydengård, M. Mörgelin, and A. Schmidtchen.** 2005. Domain 5 of high molecular weight kininogen is antibacterial. *J Biol Chem* **280**:34832-34839.

30. **Nordahl, E. A., V. Rydengård, P. Nyberg, D. P. Nitsche, M. Mörgelin, M. Malmsten, L. Björck, and A. Schmidtchen.** 2004. Activation of the complement system generates antibacterial peptides. *Proc Natl Acad Sci U S A* **101**:16879-16884.
31. **Papareddy, P., V. Rydengård, M. Pasupuleti, B. Walse, M. Mörgelin, A. Chalupka, M. Malmsten, and A. Schmidtchen.** 2010. Proteolysis of human thrombin generates novel host defense peptides. *PLoS Pathog* **6**:e1000857.
32. **Pasupuleti, M., A. Chalupka, M. Mörgelin, A. Schmidtchen, and M. Malmsten.** 2009. Tryptophan end-tagging of antimicrobial peptides for increased potency against *Pseudomonas aeruginosa*. *Biochim Biophys Acta* **1790**:800-808.
33. **Pasupuleti, M., A. Schmidtchen, A. Chalupka, L. Ringstad, and M. Malmsten.** 2009. End-tagging of ultra-short antimicrobial peptides by W/F stretches to facilitate bacterial killing. *PLoS One* **4**:e5285.
34. **Pasupuleti, M., B. Walse, E. A. Nordahl, M. Mörgelin, M. Malmsten, and A. Schmidtchen.** 2007. Preservation of antimicrobial properties of complement peptide C3a, from invertebrates to humans. *J Biol Chem* **282**:2520-2528.
35. **Pasupuleti, M., B. Walse, B. Svensson, M. Malmsten, and A. Schmidtchen.** 2008. Rational design of antimicrobial C3a analogues with enhanced effects against Staphylococci using an integrated structure and function-based approach. *Biochemistry* **47**:9057-9070.
36. **Pollock, J. S., U. Forstermann, J. A. Mitchell, T. D. Warner, H. H. Schmidt, M. Nakane, and F. Murad.** 1991. Purification and characterization of particulate endothelium-derived relaxing factor synthase from cultured and native bovine aortic endothelial cells. *Proc Natl Acad Sci U S A* **88**:10480-10484.
37. **Ringstad, L., A. Schmidtchen, and M. Malmsten.** 2006. Effect of Peptide Length on the Interaction between Consensus Peptides and DOPC/DOPA Bilayers. *Langmuir* **22**:5042-5050.
38. **Rosenfeld, Y., N. Papo, and Y. Shai.** 2006. Endotoxin (lipopolysaccharide) neutralization by innate immunity host-defense peptides. Peptide properties and plausible modes of action. *J Biol Chem* **281**:1636-1643.
39. **Rydengård, V., E. Andersson Nordahl, and A. Schmidtchen.** 2006. Zinc potentiates the antibacterial effects of histidine-rich peptides against *Enterococcus faecalis*. *Febs J* **273**:2399-2406.
40. **Sajjan, U. S., L. T. Tran, N. Sole, C. Rovaldi, A. Akiyama, P. M. Friden, J. F. Forstner, and D. M. Rothstein.** 2001. P-113D, an antimicrobial peptide active

- against *Pseudomonas aeruginosa*, retains activity in the presence of sputum from cystic fibrosis patients. *Antimicrob Agents Chemother* **45**:3437-3444.
41. **Schmidtchen, A., M. Pasupuleti, M. Morgelin, M. Davoudi, J. Alenfall, A. Chalupka, and M. Malmsten.** 2009. Boosting antimicrobial peptides by hydrophobic oligopeptide end tags. *J Biol Chem* **284**:17584-17594.
 42. **Sjogren, H., and S. Ulvenlund.** 2005. Comparison of the helix-coil transition of a titrating polypeptide in aqueous solutions and at the air-water interface. *Biophys Chem* **116**:11-21.
 43. **Steinstraesser, L., U. Kraneburg, F. Jacobsen, and S. Al-Benna.** 2011. Host defense peptides and their antimicrobial-immunomodulatory duality. *Immunobiology*. **216**:322-333
 44. **Taboureau, O., O. H. Olsen, J. D. Nielsen, D. Raventos, P. H. Mygind, and H. H. Kristensen.** 2006. Design of novispirin antimicrobial peptides by quantitative structure-activity relationship. *Chem Biol Drug Des* **68**:48-57.
 45. **van der Does, A. M., H. Beekhuizen, B. Ravensbergen, T. Vos, T. H. Ottenhoff, J. T. van Dissel, J. W. Drijfhout, P. S. Hiemstra, and P. H. Nibbering.** LL-37 directs macrophage differentiation toward macrophages with a proinflammatory signature. *J Immunol* **185**:1442-1449.
 46. **van der Poll, T., and J. C. Meijers.** 2010. Systemic inflammatory response syndrome and compensatory anti-inflammatory response syndrome in sepsis. *J Innate Immun* **2**:379-380.
 47. **Wiegand, I., K. Hilpert, and R. E. Hancock.** 2008. Agar and broth dilution methods to determine the minimal inhibitory concentration (MIC) of antimicrobial substances. *Nat Protoc* **3**:163-175.
 48. **Zanetti, M.** 2004. Cathelicidins, multifunctional peptides of the innate immunity. *J Leukoc Biol* **75**:39-48.

Figure legends

FIG. 1. Antibacterial and hemolytic activities of PEP screen peptides. (A) Composite figure indicating antimicrobial activity against *E. coli* and hemolysis (in %). The peptides (100 μ M) were tested for antimicrobial activity in low-salt and high-salt conditions in RDA against *E. coli* ATCC 25922. The bar diagram indicate the zones of clearance obtained (in mm). Hemolytic effects were investigated by incubating the cells with 60 μ M of the peptides. 2% Triton X-100 served as positive control. The absorbance of hemoglobin release is expressed as % of Triton X-100 induced hemolysis. Error bars represent the standard error of the mean (n=3). (B) Antimicrobial activities of peptides (at 100 μ M in RDA) against *P. aeruginosa* ATCC 27853, *S. aureus* ATCC 29213, and *Candida albicans* ATCC 90028.

FIG. 2. Activities of K-S variant peptides. Antimicrobial activity (in RDA) of peptides (all at 100 μ M) having lysine replaced by serine against *E. coli* ATCC25922, *P. aeruginosa* ATCC 27853, and *S. aureus* ATCC 29213 are shown. The bar diagram indicate the zones of clearance obtained (in mm).

FIG. 3. Immunomodulatory activities *in vitro*. Effects on NO production. (A) RAW 264.7 macrophage cells were stimulated with LPS from *E. coli*, LTA from *S. aureus*, and zymosan A from *Saccharomyces cerevisiae*, with and without addition of 10 μ M of peptide. NO production in the culture media 24 h after the treatment was determined using the Griess reagent.

FIG. 4. Antimicrobial activities of selected peptides at physiological conditions. (A) Minimal inhibitory concentrations (MIC) of peptides for different strains of *E. coli* and *S. aureus* are indicated. The graph shows the sum of strains exhibiting the respective MIC breakpoint (in μ M). (B) Antibacterial effects of the indicated peptides against *E. coli* ATCC 25922 in viable count assay are presented. Bacteria were incubated in 50 μ l with the indicated peptides at 0.3-60 μ M in 10 mM Tris, pH 7.4, 0.15 M NaCl (left panel) or the same buffer containing 20% human plasma (right panel). Identical buffers without peptides were used as controls.

FIG. 5. Immunomodulatory activities of selected peptides. (A) Dose dependent inhibitory effects on NO production by RAW 264.7 macrophage cells stimulated by LPS are evaluated. Cells were stimulated with LPS from *E. coli* (10 ng/ml), with and without addition of the indicated peptides at 0.5-50 μ M. NO production in the culture media 24 h after the treatment was determined using the Griess reagent. LPS-stimulated cells without peptide were used as control. LL-37 is shown for comparison. (B) Peptide effects on NO production of macrophages subjected to LTA or zymosan. GKY25 and LL37 are presented for comparison. Unstimulated and stimulated cells served as negative and positive controls, respectively.

FIG. 6. Activities of peptides against eukaryotic cells. (A) Hemolytic effects of the indicated variant peptides were investigated, and corresponding data for LL-37 are included for comparison. The cells were incubated with the peptides at 60 μ M and 120 μ M, 2% Triton X-100 served as positive control. The absorbance of hemoglobin release was measured at 540 nm and is expressed as % of Triton X-100 induced hemolysis (note scale of y-axis). (B) Effects of peptides on HaCaT cells in absence (left panel) and presence of human serum (right panel). The MTT-assay (upper panel) was used to measure viability of HaCaT keratinocytes at 30 μ M and 60 μ M in absence of human serum, and at 60 μ M in the presence of. In the assay, MTT is modified into a dye, blue formazan, by enzymes associated with metabolic activity. The absorbance of the dye was measured at 550 nm. Cell permeabilizing effects of the indicated peptides (lower panels) were measured by the LDH based TOX-7 kit. LDH release from the cells was measured at 490 nm and was plotted as % of total LDH release. (C) Effects of peptides on human skin fibroblasts. The MTT-assay (left panel) was used to measure viability of fibroblasts in the presence of the indicated peptides at 60 μ M in absence of human serum. Cell permeabilizing effects of the indicated peptides (right panel) were measured by the LDH based TOX-7 kit as above.

FIG. 7. Activities of GKY25 and GKY20 in human blood infected by bacteria. (A) Hemolysis in human blood (made 50% in PBS) in presence of the indicated bacteria as well as peptides. Hemolysis was assessed after 1 hour. (B) In an identical setup, antibacterial effects of the indicated peptides were studied. *S. aureus* and *P. aeruginosa* were added to 50% citrate blood, followed by addition of peptide at 60 or 120 μ M. The number of cfu was determined after an incubation period of 1 hour.

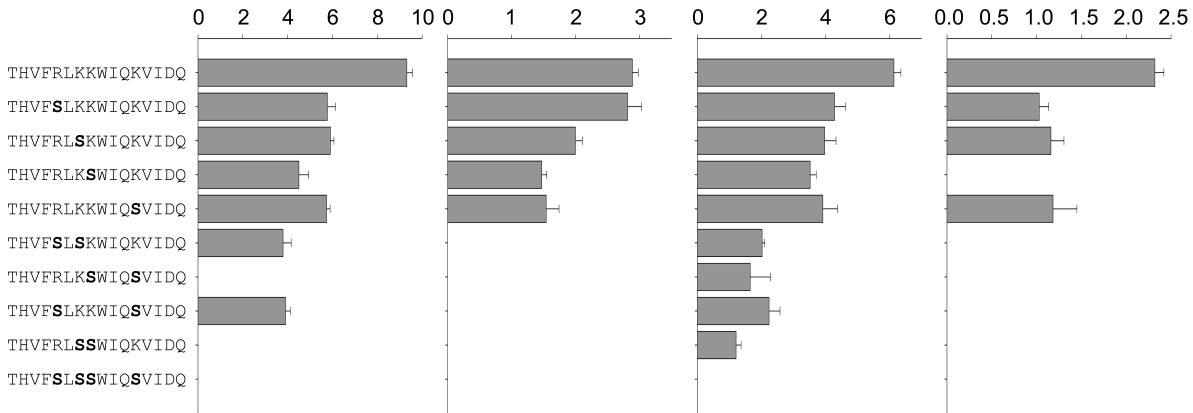
FIG. 8. Permeabilization effects and structure of peptides (A) Permeabilizing effects of peptides on *E. coli*. Bacteria were incubated with the indicated peptides and permeabilization was assessed using the impermeant probe FITC. (B) Electron microscopy analysis. *P. aeruginosa* and *S. aureus* bacteria was incubated for 2 h at 37°C with 30 μ M of GK Y20 and analyzed with electron microscopy. Scale bar represents 1 μ m. Control; Buffer control. (C) CD spectra of the indicated peptides in Tris-buffer and in presence of LPS or anionic liposomes. (D) Helical content of GK Y25, GK Y20, or VFR12 in presence of negatively charged liposomes (PA). (E) Effects of the indicated peptides on liposome leakage. The membrane permeabilizing effect was recorded by measuring fluorescence release of carboxyfluorescein from PA (negatively charged) liposomes. The experiments were performed in 10 mM Tris-buffer. Values represents mean of triplicate samples.

Figure 9. *In vivo* effects of GK Y20. (A) GK Y20 suppresses bacterial dissemination to the spleen, liver and kidney. Mice were injected i.p. with *P. aeruginosa* bacteria, followed by i.p. injection of GK Y20 or buffer only, and the cfu of *P. aeruginosa* in spleen, liver, and kidney was determined after a time period of 12 h (x=10 for controls and treated, P<0.05 for spleen, liver and kidney. Horizontal line indicates median value). (B) GK Y20 significantly increases survival in LPS-induced shock. Mice were injected with LPS followed by intraperitoneal administration of GK Y20 (200 or 500 μ g). Survival was followed for 7 days. (n=10 for controls, n=10 for treated animals, P<0.001) (left panel). Weight of the animals is indicated (middle panel). (C) GK Y20 increases thrombocytes. In a separate experiment, mice were sacrificed 20 h after i.p. injection of LPS followed by treatment with GK Y20 (500 μ g) or buffer, and thrombocytes were analyzed in blood. (D) As in (C), but the indicated cytokines were analyzed in blood (n=10 for controls, n=10 for treated animals, the P values for the respective cytokines are IL-6, 0.001; IFN- γ =0.009; TNF, 0.001; IL-12p70, 0.001. IL-10 was increased. (E) Lungs were analyzed 20 h after LPS injection i.p. followed by treatment with GK Y20 (500 μ g) or buffer. Histochemical analysis shows marked attenuation of inflammatory changes in GK Y20-treated lungs (a representative lung section is shown). (F) Lungs were analyzed by scanning electron microscopy 20 h after LPS injection i.p., followed by treatment with GK Y20 (500 μ g) or buffer. Treatment with the peptide blocked leakage of proteins and erythrocytes (n=3 in both groups, and a representative lung section is shown).

*E. coli**P. aeruginosa**S. aureus*

Zone of inhibition (mm)

+0.15M NaCl



LPS

LTA

Zymosan

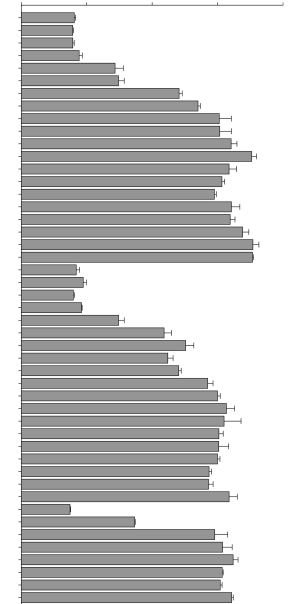
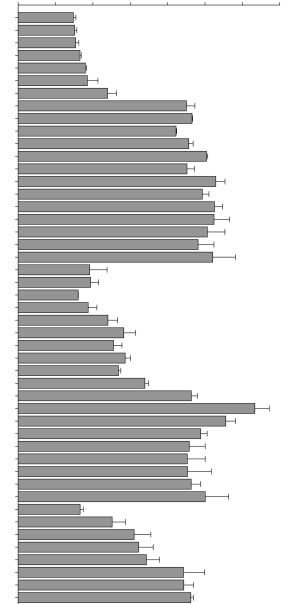
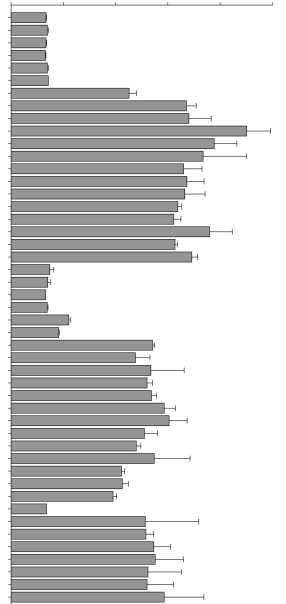
Nitrate (μM)

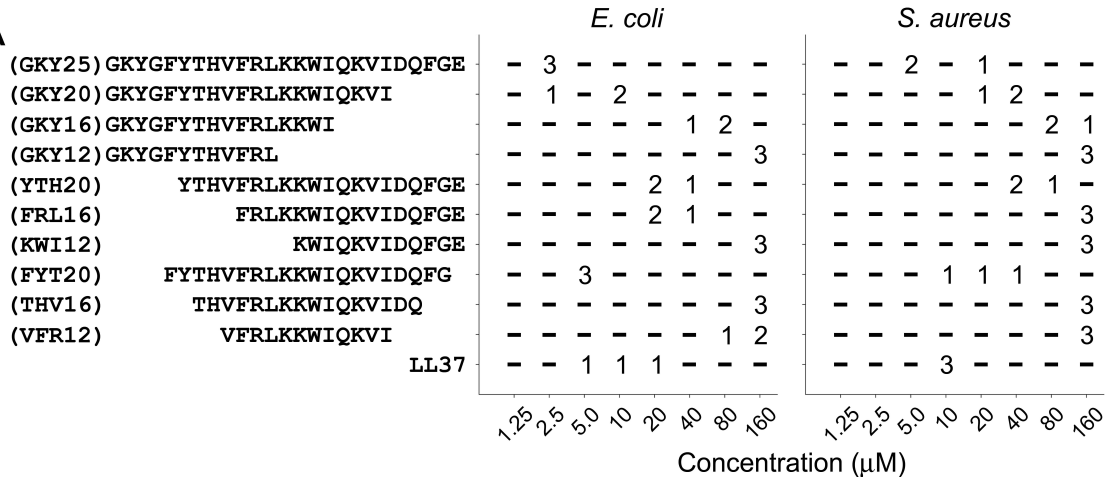
0 5 10 15 20 25

0 5 10 15 20 25 30 35

0 10 20 30 40

GKYGfYTHVfRLKKWIQKVIDQFGE
 GKYGfYTHVfRLKKWIQKVIDQFG
 GKYGfYTHVfRLKKWIQKVIDQF
 GKYGfYTHVfRLKKWIQKVIDQ
 GKYGfYTHVfRLKKWIQKVID
 GKYGfYTHVfRLKKWIQKVI
 GKYGfYTHVfRLKKWIQKV
 GKYGfYTHVfRLKKWIQK
 GKYGfYTHVfRLKKWIQ
 GKYGfYTHVfRLKKWI
 GKYGfYTHVfRLKKW
 GKYGfYTHVfRLKK
 GKYGfYTHVfRLK
 GKYGfYTHVfRL
 GKYGfYTHVfR
 GKYGfYTHVf
 GKYGfYTHV
 GKYGfYTH
 GKYGfYT
 GKYGfY
 KYGfYTHVfRLKKWIQKVIDQFGE
 YGfYTHVfRLKKWIQKVIDQFGE
 GfYTHVfRLKKWIQKVIDQFGE
 FYTHVfRLKKWIQKVIDQFGE
 YTHVfRLKKWIQKVIDQFGE
 THVfRLKKWIQKVIDQFGE
 HVfRLKKWIQKVIDQFGE
 VfRLKKWIQKVIDQFGE
 RfRLKKWIQKVIDQFGE
 RLKKWIQKVIDQFGE
 LKKWIQKVIDQFGE
 KKWIQKVIDQFGE
 KWIQKVIDQFGE
 WIQKVIDQFGE
 IQKVIDQFGE
 QKVIDQFGE
 KVfIDQFGE
 VIfIDQFGE
 IIfIDQFGE
 FYTHVfRLKKWIQKVIDQFG
 YTHVfRLKKWIQKVIDQF
 THVfRLKKWIQKVIDQ
 HVfRLKKWIQKVID
 VfRLKKWIQKVI
 RfRLKKWIQKV
 RLKKWIQK
 LKKWIQ



A**B**